

Article

# Method to Determine the Constitutive Permeability Parameters of Non-Linear Consolidation Models by Means of the Oedometer Test

Gonzalo García-Ros \* and Iván Alhama

Civil Engineering Department, Mining and Civil Engineering Faculty, Technical University of Cartagena, 30203 Cartagena, Spain; ivan.alhama@upct.es

\* Correspondence: gonzalo.garcia@upct.es; Tel.: 34-678-43-70-60

Received: 19 October 2020; Accepted: 15 December 2020; Published: 17 December 2020



**Abstract:** This paper presents an easy-to-apply methodology that allows obtaining the permeability index and the initial hydraulic conductivity of clayey soils, basic constitutive parameters in non-linear models of consolidation, based on the laboratory oedometer test. For this, the data of the void ratio, compressibility index and characteristic consolidation time are taken from the test and, as an inverse problem, the constitutive permeability parameters sought are determined by applying the universal solutions of the characteristic time for a general non-linear consolidation model with constitutive relations void ratio-effective soil stress and hydraulic conductivity-void ratio of logarithmic type. The application protocol of the inverse problem is described in detail and illustrated by a series of applications carried out on real laboratory data belonging to two different soils. The influence that errors in laboratory parameter measurements can have on the final values of the permeability index and initial hydraulic conductivity is studied, showing the maximum deviations that may appear and, by last, the precision of the results obtained.

**Keywords:** inverse problem; constitutive permeability parameters; non-linear consolidation; oedometer test; universal consolidation curves

## 1. Introduction

The determination of the constitutive parameters that govern the consolidation of soils is a topic of great interest in geotechnics in order to calculate the characteristic time of the process, as well as the evolution of the degree of consolidation and the surface settlement [1,2].

It is known that the solutions to the consolidation problem derived from the universal linear consolidation curves [3] always fall on the side of safety when designing a soil consolidation project, hence the widespread use of these curves. However, in most soils, the hypotheses assumed by the linear theory are severe and the deviations of its analytical solutions from the experimental results can be appreciable, reaching relative errors that are close and even greater than 100% [4]. In order to study the non-linear behavior, different types of dependency between porosity (void ratio) and effective stress, on the one hand, and hydraulic conductivity and effective stress (or porosity), on the other, have been proposed in the scientific literature over the last decades. These dependencies conform to logarithmic and potential functions, and their authors name the type of non-linear consolidation that derives from them. The most widespread models are those of Davis and Raymond [5], Juárez-Badillo [6] and Cornetti and Battaglio [7], the last reformulated by Arnod et al. [8]. Among the hypotheses assumed by these models we highlight the incompressibility of the fluid and the soil skeleton, a constant volume  $(1 + e)$  in the term of soil compression in the equilibrium equation and the non-consideration of creep effects [9,10]. The most commonly used model in the literature, Cornetti and Battaglio [7],

assumes logarithmic type dependencies both between the void ratio and the effective stress and between the void ratio and the hydraulic conductivity.

Recently, the dimensionless groups that characterize the aforementioned models, as well as their extensions to more general and precise formulations obtained from the elimination of several restrictive hypotheses [11], have been derived from their governing equations and the application of the pi theorem [12], which has allowed the construction of universal curves of easy use for the determination of the characteristic consolidation time, the average degree of pressure dissipation and the average degree of settlement [13–16]. The results obtained by these authors reduce the numerous coefficients (dimensional or not) involved in the models to a small number of dimensionless groups based on which the solution for each unknown is presented by a single universal curve. For the purpose of this article, the consolidation model used is that of Alhama et al. [15], an extension of Cornetti and Battaglio [7] in which the restrictive hypotheses of constant volume in the contraction term of the governing equation and constant thickness of the volume element along the consolidation process have been deleted.

In the present paper, based on the results of a simple oedometer test and making use of the universal solutions of the Alhama et al. model [15], the constitutive soil parameters that characterize this are determined. These are:  $C_c$  (compression index),  $c_k$  (permeability index) and  $k_o$  (initial hydraulic conductivity). For this, the universal curve of the characteristic time to reach 90% of the final settlement ( $\tau_{0.9}$ ), a parameter of clear physical meaning [15,17], is used.

The proposed work falls into the category of so-called inverse engineering problems [18–22] since it is based on experimental data to infer, in this case, the properties of the soil [23,24]. The consolidation curves associated with two successive step loads (in accordance with the standards of the oedometer test) allow to obtain directly both the compression index and the characteristic time of settlement of each curve. With these last data, the universal curves of the model allow to adjust graphically, or analytically through simple mathematical programming routines, the values of the rest of the parameters sought, that is,  $c_k$  and  $k_o$ .

In addition to the great precision in the estimation of these parameters, it was analyzed the influence of the errors that can occur in the reading of the data coming from the oedometer test: the characteristic consolidation time and the compression index. For this purpose, these parameters were affected by errors of 0.5, 1 and 2% and, after applying again the calculation routine to obtain  $k_o$  and  $c_k$ , their deviations were quantified, always being less than 20%. This maximum value is considerably reduced when, as in reality, the errors made are random for the same maximum instrumental error.

In the following, the mathematical non-linear consolidation model of Alhama et al. [15] is presented first, then collecting the dimensionless groups that govern it and the universal curve corresponding to the characteristic consolidation time. Next, the inverse problem statement and the protocol proposed for its solution are described, then solving two applications with real data from both oedometer tests corresponding to a clayey soil with a high content of muscovite and a kaolinite. An analysis of the influence of errors (calibration or reading) of the oedometer test data is made and, finally, we find a section that summarizes the contributions and conclusions of the work.

## 2. Non-Linear Consolidation Mathematical Model, Dimensionless Groups and Universal Curves

The following summarizes the deduction of the non-linear consolidation equation and the dimensionless groups derived from the model of Alhama et al. [15], which is a generalization of the Cornetti and Battaglio [7] model by elimination of the restrictive hypotheses of constant volume in the contraction term of the governing equation and constant thickness of the volume element along the consolidation process.

The constitutive dependencies  $e = e(\sigma')$  and  $e = e(k)$  for the Alhama et al. model [15] are:

$$e = e_o - C_c \log_{10} \left( \frac{\sigma'}{\sigma'_o} \right) \text{ or } \sigma' = \sigma'_o 10^{-\left( \frac{e - e_o}{C_c} \right)} \quad (1)$$

$$e = e_0 + c_k \log_{10}\left(\frac{k}{k_0}\right) \text{ or } k = k_0 10^{\left(\frac{e-e_0}{c_k}\right)} \tag{2}$$

From these, the dependency  $k = k(\sigma')$  is given by

$$k = k_0 \left(\frac{\sigma'}{\sigma'_0}\right)^{-\frac{c_c}{c_k}} = k_0 \left(\frac{\sigma'}{\sigma'_0}\right)^{\lambda-1} \text{ being } \lambda = 1 - \frac{c_c}{c_k} \tag{3}$$

The balance equation for a volume element equals the change in the void ratio per unit time to the flow of water leaving the element. Its expression, if we eliminate the restrictive hypothesis of constant volume  $(1 + e)$  in the term of soil compression, is

$$\frac{\partial}{\partial z} \left( \frac{k(u)}{\gamma_w} \frac{\partial u}{\partial z} \right) = \frac{\partial}{\partial t} \left( \frac{e}{(1+e)} \right) = \frac{1}{(1+e)^2} \left( \frac{\partial e}{\partial t} \right) \tag{4}$$

Taking into account the relation between the excess pore pressure and the effective stress of the soil,

$$\sigma' = \sigma_c - u + \sigma'_0 \tag{5}$$

Equation (4) can be developed (using the Equations (1), (2), (3) and (5) conveniently) and written in terms of the excess pore pressure

$$\frac{\partial u}{\partial t} = \frac{(1+e)^2 L(10) \sigma'_0 k_0}{C_c \gamma_w} \left( \frac{\sigma_c - u + \sigma'_0}{\sigma'_0} \right)^\lambda \left[ \left( \frac{\partial^2 u}{\partial z^2} \right) + \left( \frac{1-\lambda}{\sigma_c - u + \sigma'_0} \right) \left( \frac{\partial u}{\partial z} \right)^2 \right] \tag{6}$$

or, if preferred, in terms of the effective pressure

$$\frac{\partial \sigma'}{\partial t} = \frac{(1+e)^2 L(10) \sigma'_0 k_0}{C_c \gamma_w} \left( \frac{\sigma'}{\sigma'_0} \right)^\lambda \left[ \left( \frac{\partial^2 \sigma'}{\partial z^2} \right) - \left( \frac{1-\lambda}{\sigma'} \right) \left( \frac{\partial \sigma'}{\partial z} \right)^2 \right] \tag{7}$$

Alternatively, the consolidation equation can also be written in terms of the new variable  $\omega = e - e_f$ , with a clear physical meaning and directly related to the degree of settlement. Through the constitutive dependency  $e - \sigma'$ , and after a series of mathematical manipulations, is reached

$$\frac{\partial \omega}{\partial t} = \frac{(1+e)^2 L(10) \sigma'_0 k_0}{C_c \gamma_w} \left( \frac{\sigma'}{\sigma'_0} \right)^\lambda \left[ \left( \frac{\partial^2 \omega}{\partial z^2} \right) - \lambda \frac{L(10)}{I_c} \left( \frac{\partial \omega}{\partial z} \right)^2 \right] \tag{8}$$

In addition, the hypothesis of assuming variable the thickness of the volume element leads to a dependency relation between  $dz$  and  $e$ , given by

$$dz = dz_0 \frac{1+e}{1+e_0} \tag{9}$$

In summary, the non-linear mathematical model is formed by the governing Equations (6), or (7) or (8) and (9), plus the constitutive dependencies and definitions above. To these, the necessary initial and boundary conditions must be added. The transformation of these governing equations to their dimensionless forms allows the deduction of the dimensionless groups that govern the solution of the problem, which for the case studied in terms of settlements (8) are reduced to only two. These are:

$$\pi_I = \frac{\tau_{0.9} (1+e_0)^2 \sigma'_0 k_0}{C_c \gamma_w H_0^2}, \pi_{II} = \left( \frac{\sigma'_f}{\sigma'_0} \right)^\lambda \tag{10}$$

The pi theorem allows to write the relation between the characteristic time (through the dimensionless monomial  $\pi_I$  in which this time is defined) and the dimensionless group  $\pi_{II}$ , in the form  $\pi_I = \Psi(\pi_{II})$  or

$$\tau_{0.9} = \frac{C_c \gamma_w H_o^2}{(1 + e_o)^2 \sigma'_o k_o} \Psi \left[ \left( \frac{\sigma'_f}{\sigma'_o} \right)^\lambda \right] \tag{11}$$

The unknown function  $\Psi$  was determined and verified through numerical simulations, providing the universal curve shown in Figure 1.

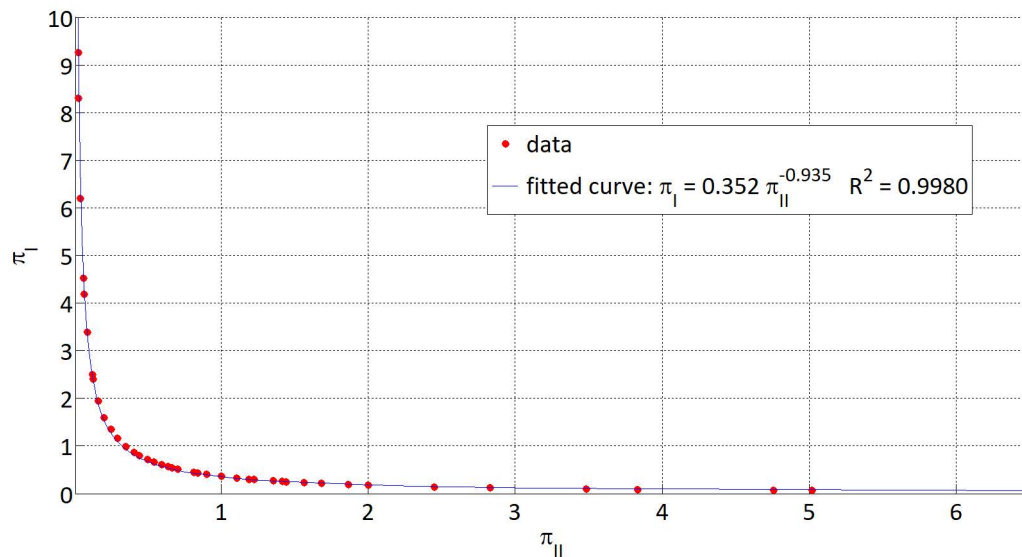


Figure 1. Universal curve  $\pi_I = \Psi(\pi_{II})$ . Alhama et al. [15].

The authors also adjusted this dependency, covering a wide range of values of the monomials  $\pi_I$  and  $\pi_{II}$  around unit (which in fact covers all cases of interest in practice), to a potential function with regression coefficient 0.9980. They also reported a finer adjustment of this function, with regression coefficients very close to the unit, separating the curve into three sections. The results are given by the following expressions:

$$\pi_I = 0.352 \pi_{II}^{-0.935} \quad \pi_I \in [0, 10] \quad \pi_{II} \in [0, 6.5] \quad R^2 = 0.9980 \tag{12}$$

$$\pi_I = 0.413 \pi_{II}^{-0.868} \quad \pi_I \in [2, 14] \quad \pi_{II} \in [0.02, 0.16] \quad R^2 = 0.9997 \tag{13}$$

$$\pi_I = 0.374 \pi_{II}^{-0.930} \quad \pi_I \in [0.4, 2] \quad \pi_{II} \in [0.16, 1] \quad R^2 = 0.9997 \tag{14}$$

$$\pi_I = 0.373 \pi_{II}^{-1.047} \quad \pi_I \in [0.05, 0.4] \quad \pi_{II} \in [1, 6.5] \quad R^2 = 0.9998 \tag{15}$$

### 3. Parameter Calculation Protocol

As we have mentioned, it is based on a soil sample of known initial thickness (or draining length  $H_o$ ), void ratio ( $e_o$ ) and effective stress ( $\sigma'_o$ ). After performing an oedometer test and representing two of its consecutive consolidation curves, the parameters characteristic settlement time ( $\tau_{0.9}$ ) and compression index ( $C_c$ ) for each step load are determined (the compression index will be very similar in both steps). With these values and the universal characteristic time curve, the initial hydraulic conductivity ( $k_o$ ) and the permeability index ( $c_k$ ) are obtained. In detail, the proposed protocol is broken down into the following steps:

- (i) A sample of normally consolidated soil, from which we know its initial parameters  $e_o$ ,  $H_o$  and  $\sigma'_o$ , is selected. With it, the oedometer test is prepared to obtain two successive consolidation curves,  $H = H(t)$ . The effective stresses  $\sigma'_1$  (final effective stress of the first step and initial effective

stress of the second) and  $\sigma'_2$  (final effective stress of the second step) applied to the sample are set. Although not mandatory, the provisions of the oedometer standard are followed as regards the ratio of loads for a certain step, so that  $\sigma'_1 = 2\sigma'_0$  and  $\sigma'_2 = 2\sigma'_1$ .

- (ii) From the previous consolidation curves and using, for example, the graphic method of Casagrande [25], the final thicknesses of the sample (or final draining lengths  $H_1$  and  $H_2$ ) due to primary consolidation are determined and, from these and the H-e relation  $\frac{H}{H_0} = \frac{1+e}{1+e_0}$ , the final void ratios of primary consolidation ( $e_1$  and  $e_2$ , respectively) are also noted. The characteristic times of each stage,  $\tau_{0,9,1}$  and  $\tau_{0,9,2}$ , which are different due to the non-linearity of the problem, are defined as those elapsed from the beginning of each stage until the sample reaches 90% of the total range of thickness reduction by primary consolidation. This is the time with which the universal consolidation curves are constructed [15]. So,  $\tau_{0,9,1}$  reads at the point  $H = H_0 - 0.9(H_0 - H_1)$  in the first curve while  $\tau_{0,9,2}$  at  $H = H_1 - 0.9(H_1 - H_2)$  in the second.
- (iii) From the segments of the oedometric curve defined by the pairs  $(e_0, \sigma'_0)$  and  $(e_1, \sigma'_1)$ , and  $(e_1, \sigma'_1)$  and  $(e_2, \sigma'_2)$ , the compression index of each step is determined.  $C_{c,1} = (e_1 - e_0) / (\log_{10}\{\sigma'_0\} - \log_{10}\{\sigma'_1\})$  and  $C_{c,2} = (e_2 - e_1) / (\log_{10}\{\sigma'_1\} - \log_{10}\{\sigma'_2\})$ . As expected, both indices must be nearly the same,  $C_{c,1} \cong C_{c,2}$ . So far, we have the following parameters: the effective stresses  $\sigma'_0, \sigma'_1, \sigma'_2$ , the draining lengths  $H_0, H_1, H_2$ , the void ratios  $e_0, e_1, e_2$ , the characteristic times  $\tau_{0,9,1}, \tau_{0,9,2}$  and the compression indexes  $C_{c,1}, C_{c,2}$ .
- (iv) The following steps really constitute a relatively simple inverse problem that allows determining, using the characteristic time curves, the permeability index  $c_k$  and initial hydraulic conductivity of the soil  $k_o$ , as well as, from them, the hydraulic conductivities  $k_1$  and  $k_2$  at the end of each consolidation stage.
- (v) An initial hydraulic conductivity value is set,  $k_{o,I}$ .
- (vi) From  $k_{o,I}, C_{c,1}, \tau_{0,9,1}$  and the rest of the parameters involved in  $\pi_I$  and  $\pi_{II}$  ( $e_0, H_0, \sigma'_0, \sigma'_1$  and  $\gamma_w$ ), the universal Equation (12) is solved to obtain a first value of the permeability index,  $c_{k,I}$ .
- (vii) With  $k_{o,I}, c_{k,I}, C_{c,1}, \sigma'_0$  and  $\sigma'_1$ , using the dependency (3), the final hydraulic conductivity of the first compressibility curve (or the initial one of the second) is calculated. Let us call this conductivity  $k_{1,I}$ . Now, from  $k_{1,I}, C_{c,2}, c_{k,I}$  and the parameters  $e_1, H_1, \sigma'_1, \sigma'_2$  and  $\gamma_w$ , Equation (12) provides a characteristic time  $\tau_{0,9,2,I}$ .
- (viii) Calculate the simple functional defined by

$$\Theta_I = \frac{\tau_{0,9,2,I}}{\tau_{0,9,2}} \tag{16}$$

This value will generally be much greater than unit if high initial hydraulic conductivities (of the order of  $k_{o,I} = 10^{-7}$ ) are chosen, or much smaller than unit if low ones are taken (of the order of  $k_{o,I} = 10^{-13}$ ). We will assume that we have chosen a high initial hydraulic conductivity, so that  $\Theta_I \gg 1$ .

- (i) Repeat steps (v) to (vii) for the successive values of initial hydraulic conductivity  $0.1k_{o,I}, 0.01k_{o,I}, 0.001k_{o,I} \dots$  and determine their respective resulting functionals. These functionals will decrease monotonously until for a given one whose value is lower than unit. Then, we retain the value of the last conductivity whose functional was above the unit, as well as its associated permeability index and functional value. Let  $k_{o,F,I}, c_{k,F,I}$  and  $\Theta_{F,I}$  be these values.
- (ii) If  $\Theta_{F,I} < \Theta_{ref}$  (a sufficiently small reference value, for example  $\Theta_{ref} = 1.001$ ),  $k_{o,F,I}$  and  $c_{k,F,I}$  are the solutions sought. If  $\Theta_{F,I} > \Theta_{ref}$ , rename  $k_{o,F,I}$  as  $k_{o,I}$  and go to step x).
- (iii) Repeat the steps (v) to (vii) for initial conductivities  $0.9k_{o,I}, 0.8k_{o,I}, 0.7k_{o,I}, \dots, 0.1k_{o,I}$  and determine their resulting functionals. Again, the functional value will decrease until being lower than unit and we will retain the value of the last conductivity whose functional was above the unit, as well as its associated value of  $c_k$ . Let  $k_{o,F,I}, c_{k,F,I}$  and  $\Theta_{F,I}$  be these values. If  $\Theta_{F,I} < \Theta_{ref}$ ,  $k_{o,F,I}$  and  $c_{k,F,I}$  are the solutions sought. If  $\Theta_{F,I} > \Theta_{ref}$ , rename  $k_{o,F,I}$  as  $k_{o,I}$  and repeat this step.

- (iv) If in step (x) it happens that the functional for  $0.9k_{o,I}$  is less than one, then we will reduce the conductivity as follows:  $0.99k_{o,I}, 0.98k_{o,I}, 0.97k_{o,I}, \dots, 0.9k_{o,I}$ . Once we have found the value of  $k_{o,EI}$  of this step, if  $\Theta_{F,I} > \Theta_{ref}$  we rename again  $k_{o,EI}$  as  $k_{o,I}$  and we continue iterating, this time the way  $0.999k_{o,I}, 0.998k_{o,I}, 0.997k_{o,I}, \dots, 0.99k_{o,I}$ . We will use this methodology on a recurring basis until  $\Theta_{F,I} < \Theta_{ref}$ , moment in which we will have determined the definitive values of  $k_o$  and  $c_k$ .

A similar procedure could be established if we start with a low hydraulic conductivity value that will increase until we converge on the same solution. It should be noted, on the one hand, that Equations (13) to (15) can replace (12) in step (vi), in order to increase the reliability of the solutions of each iteration. On the other hand, as regards the step (viii) and successive, other criteria could be chosen to improve or optimize the protocol, but it is an option outside the substance of the proposed routine.

#### 4. Applications

For the experimental tests, a kaolinite and a clayey soil with a high content of muscovite have been chosen. The gradation curves of these soils are shown in Figure 2 (sedimentation method), while their mineralogical compositions, obtained by X-Ray Diffraction (XRD), are summarized in Table 1.

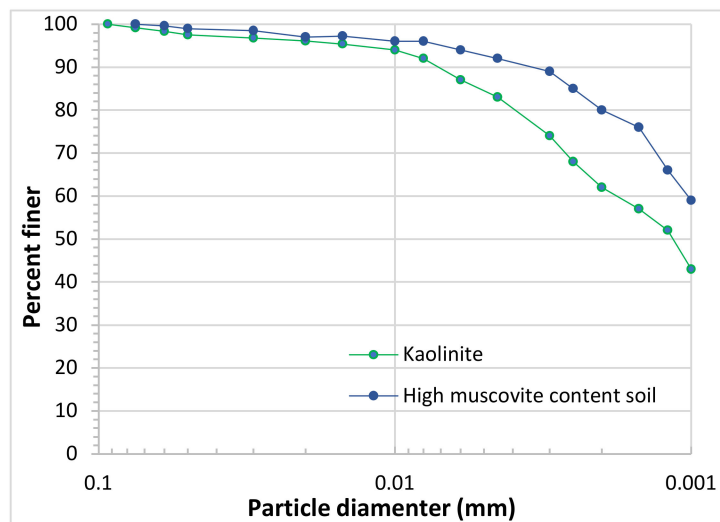


Figure 2. Grain size distribution of kaolinite and high muscovite content clayey soil.

Table 1. Mineralogical composition of the two soils tested (Oriented aggregates).

Soil	Compound Name	Formula	(%)	System	Space Group
High muscovite content soil	Kaolinite-1Ad	$Al_2Si_2O_5(OH)_4$	60	Triclinic	C1 (1)
	Muscovite-2M1	$KAl_2(Si,Al)_4O_{10}(OH)_2$	26	Monoclinic	C2/c (15)
	Quartz, low	$SiO_2$	14	Hexagonal	P3121 (152)
Kaolinite	Kaolinite-1Ad	$Al_2Si_2O_5(OH)_4$	93	Triclinic	C1 (1)
	Muscovite-2M1	$KAl_2(Si,Al)_4O_{10}(OH)_2$	7	Monoclinic	C2/c (15)

Two 11-stage oedometer compressibility tests have been performed on two remolded samples (one for each soil). The tests have been carried out according to the Spanish standard UNE-EN ISO 17892–17895 [26], following the procedure for remolded samples. For this, the confining ring (50 mm in diameter and 20 mm in height) is driven into the specimen until it is full of soil and, once the excess soil is removed, it is placed in the loading cell. Both samples were reconsolidated at an effective stress of 12.5 kPa, following the recommendations of the standard. In Table 2, the main geotechnical properties of both soils are summarized. Let us remember that in this test, unlike others such as, for example, those performed with hydraulic consolidation cells [27], pore pressure measurements are not carried

out. On the other hand, the consolidation tests were performed with drainage on both the lower and upper faces (double drainage), so that the initial draining length  $H_0$  of both samples was 10 mm (half the height of the confining ring).

**Table 2.** Geotechnical properties of the two soils tested.

Soil	$G_s$	LL	IP	Classification (SUCS)	$e_{0,r}$	$\sigma'_{o,0ed}$ (kPa)	$e_{o,0ed}$	Moisture Content (%)	Bulk Density ( $g/cm^3$ )	Free Swelling (%)
Soil with muscovite	2.72	64.39	33.14	CH-MH	1.350	12.5	1.156	43.47	1.48	5.34
Kaolinite	2.66	74.12	47.13	CH	1.214	12.5	1.073	40.34	1.65	7.21

The compressibility curves of these soils were obtained (Figures 3 and 4), as well as the consolidation curves of all loading stages, of which Figures 5–8 are illustrated, which correspond, respectively, to the normally consolidated loading steps 2, 3, 8 and 9 of the clayey soil with muscovite (and that will be used in 2 of the 4 applications presented here).

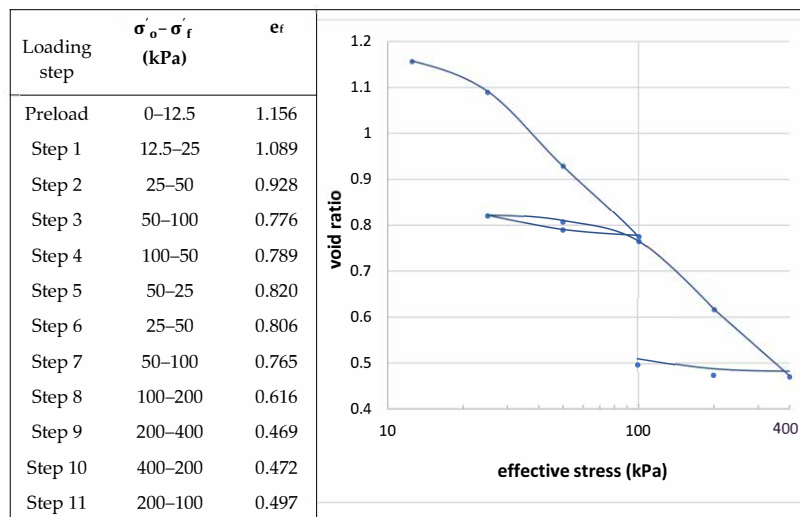


**Figure 3.** Compressibility curve of the clayey soil with a high content of muscovite.

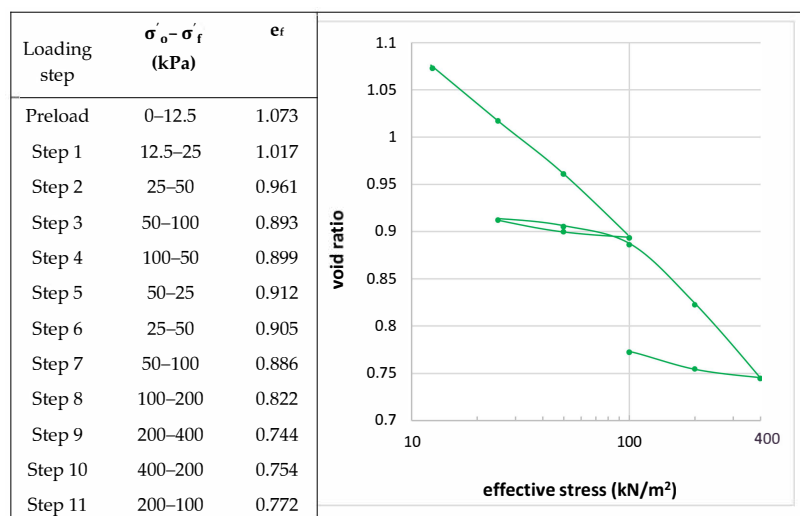


**Figure 4.** Compressibility curve of the kaolinite.

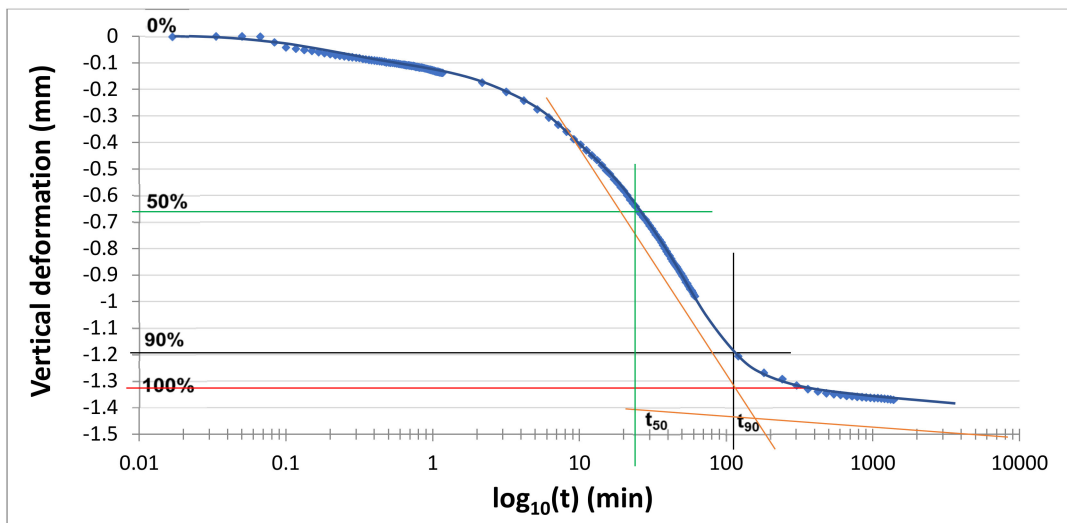


Figure 5. Consolidation curve of loading step 2 (high content muscovite soil).

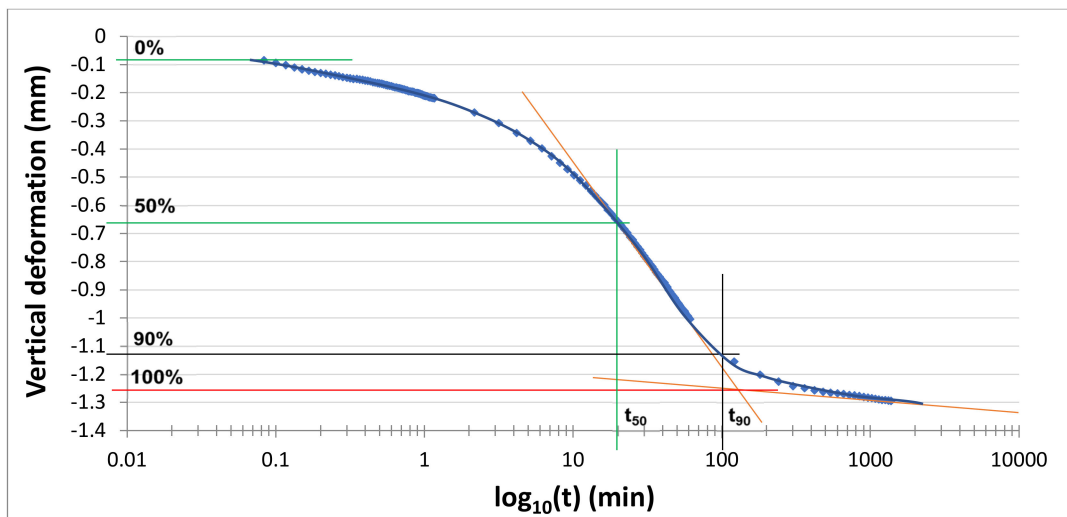


Figure 6. Consolidation curve of loading step 3 (high content muscovite soil).

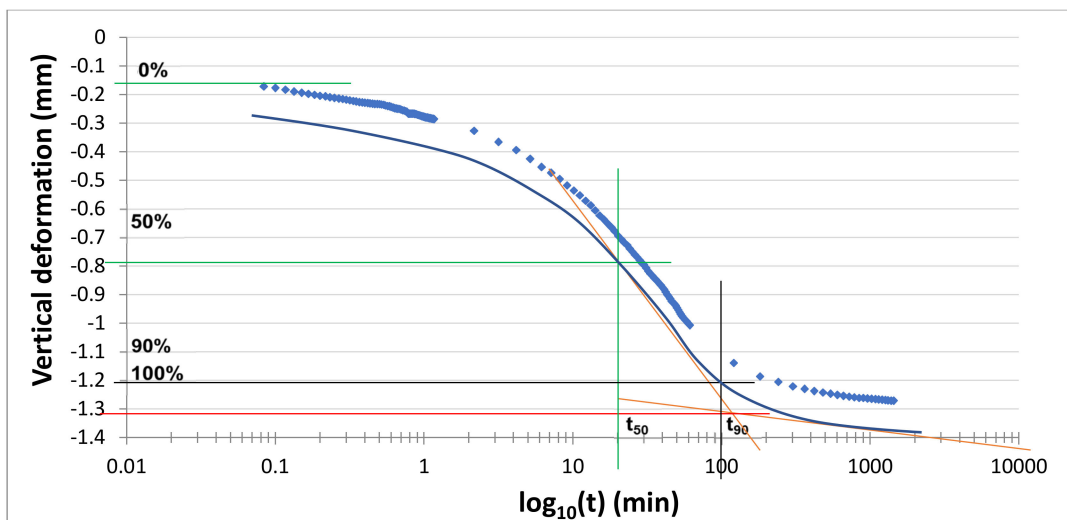


Figure 7. Consolidation curve of loading step 8 (high content muscovite soil).

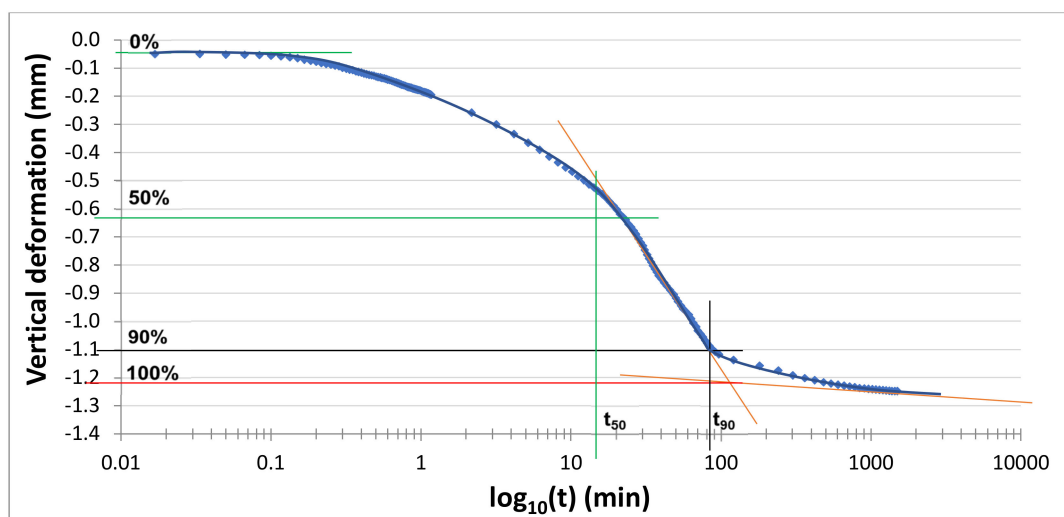


Figure 8. Consolidation curve of loading step 9 (high content muscovite soil).

#### 4.1. Applications on Clayey Soil with Muscovite

This section shows 2 applications of the proposed methodology for the determination of  $c_k$  and  $k_o$  in the clayey soil with high muscovite content: one for low levels of effective stress (between 25 and 100 kPa) and another at medium-high levels (between 100 and 400 kPa).

For the first application we will take the results of the successive steps 2 and 3 of the consolidation test, in which the sample was subjected to the following loads:

- First test (step 2): from  $\sigma'_o = 25$  kPa to  $\sigma'_1 = 2\sigma'_o = 50$  kPa.
- Second test (step 3): from  $\sigma'_1 = 50$  kPa to  $\sigma'_2 = 2\sigma'_1 = 100$  kPa.

Starting with the initial values  $H_o$  and  $e_o$  of each step (Table 3), consolidation curves (Figures 5 and 6) are used to determine the final void ratios corresponding to primary consolidation ( $e_f$ ). The application of the log t method by Casagrande and Fadum [25] to these graphs allows to obtain the sample thicknesses at the end of each primary consolidation stage (or draining lengths  $H_f$ ), deducting then the values of  $e_f$  and, consequently, the parameter  $C_c$  of each loading step (very close to each other, as expected: 0.519 for step 2 and 0.457 for step 3). The characteristic time of each stage ( $\tau_{0,9}$ ), corresponding to  $H = H_o - 0.9(H_o - H_f)$ , is obtained directly from each graph ( $t_{90}$ ): 119 and 101 min for stages 2 and 3, respectively.

Table 3. Data obtained from compressibility and consolidation curves in clayey soil with muscovite (steps 2 and 3).

Step	$\sigma'_o$ (kPa)	$\sigma'_f$ (kPa)	$S_{100}$ (mm)	$S_i$ (mm)	$S_{prim,cons}$ (mm)	$H_o$ (mm)	$H_f$ (mm)	$e_o$	$e_f$	$C_c$	$\tau_{0,9}$ (s)
2	25	50	-1.33	0	-1.33	8.891	8.226	1.089	0.933	0.519	7140
3	50	100	-1.25	-0.08	-1.17	8.166	7.581	0.919	0.781	0.457	6060

Table 3 shows a summary of the main data obtained from the consolidation tests and that we will use in the determination of  $c_k$  and  $k_o$ . At this point we highlight the significant difference that exists between the final void ratio of the first test (0.933) and the initial of the second (0.919), which is mainly due to immediate settlements ( $S_i$ ) that take place at loading application.

With all these data we proceed to step (iv) of the calculation protocol.

We assign an initial value to hydraulic conductivity,  $k_{o,I} = 10^{-7}$  m/s. Substituting this value, together with the rest of the parameters ( $C_{c,1} = 0.519$ ;  $\tau_{0,9,1} = 7,140$  s;  $e_o = 1.089$ ;  $H_o = 8.891$  mm;  $\sigma'_o = 25$  kPa;  $\sigma'_1 = 50$  kPa and  $\gamma_w = 9.8$  kN/m<sup>3</sup>), in Equation (12), a first value of the permeability index is obtained,  $c_{k,I} = 0.0483$ . With this, together with  $k_{o,I}$ ,  $C_{c,1}$ ,  $\sigma'_o$  and  $\sigma'_1$ , Equation (3) allows us to obtain

$k_{1,I} = 5.8587 \times 10^{-11}$  m/s. Using again Equation (12), from  $k_{1,I}$ ,  $c_{k,I}$ ,  $C_{c,2} = 0.457$  and the rest of the parameters ( $e_1 = 0.919$ ;  $H_1 = 8.166$  mm;  $\sigma'_1 = 50$  kPa and  $\sigma'_2 = 100$  kPa), is obtained  $\tau_{0,9,2,I} = 2.298 \times 10^6$  s. From step (vii), with  $\tau_{0,9,2} = 6,060$  s, we have  $\Theta_I = 394.8942$ . After this first iteration, we continue conveniently with the following steps of the protocol until we reach, for example,  $\Theta_{F,I} < 1.001$  (always  $\Theta_{F,I}$  being a value greater than unit).

Once the protocol is finished, the values obtained are  $k_{o,I} = 1.8400 \times 10^{-10}$  m/s (this is,  $k_o \cong 1.840 \times 10^{-10}$  m/s) and  $c_{k,I} = 0.5092$  (this is,  $c_k \cong 0.509$ ). Table 4 shows the intermediate data of the initial hydraulic conductivity, permeability index and functional along the 19 iterations that have been necessary for the convergence of the calculation process. The routine to solve Equations (3) and (12) has been programmed in MATLAB and is executed instantly.

**Table 4.** First application. Partial results of  $k_{o,I}$ ,  $c_{k,I}$  and  $\Theta_I$  throughout the iteration process.

Iteration	$k_{o,I}$ (m/s)	$c_{k,I}$	$\Theta_I$	Iteration	$k_{o,I}$ (m/s)	$c_{k,I}$	$\Theta_I$
01	$1.0000 \times 10^{-7}$	0.0483	394.8942	11	$2.0000 \times 10^{-10}$	0.4521	1.0829
02	$1.0000 \times 10^{-8}$	0.0722	44.3877	12	$1.9800 \times 10^{-10}$	0.4583	1.0726
03	$1.0000 \times 10^{-9}$	0.1429	4.9894	13	$1.9600 \times 10^{-10}$	0.4647	1.0623
04	$9.0000 \times 10^{-10}$	0.1496	4.5145	14	$1.9400 \times 10^{-10}$	0.4714	1.0520
05	$8.0000 \times 10^{-10}$	0.1579	4.0370	15	$1.9200 \times 10^{-10}$	0.4783	1.0417
06	$7.0000 \times 10^{-10}$	0.1685	3.5564	16	$1.9000 \times 10^{-10}$	0.4856	1.0314
07	$6.0000 \times 10^{-10}$	0.1826	3.0723	17	$1.8800 \times 10^{-10}$	0.4931	1.0211
08	$5.0000 \times 10^{-10}$	0.2026	2.5841	18	$1.8600 \times 10^{-10}$	0.5010	1.0108
09	$4.0000 \times 10^{-10}$	0.2341	2.0908	19	$1.8400 \times 10^{-10}$	0.5092	1.0005
10	$3.0000 \times 10^{-10}$	0.2926	1.5912				

Finally, Table 5 shows the values obtained for  $c_k$  and the different hydraulic conductivities of the soil ( $k_o$ ,  $k_1$  and  $k_2$ ) in loading steps 2 and 3.

**Table 5.** First application.  $c_k$  and initial and final hydraulic conductivities for loading steps 2 and 3.

$k_{o,step 2}$ (m/s)	$k_{f,step 2} = k_{o,step 3}$ (m/s)	$k_{f,step 3}$ (m/s)	$c_k$
$1.840 \times 10^{-10}$	$9.077 \times 10^{-11}$	$4.875 \times 10^{-11}$	0.509

In the second application, referring to the same soil, the range of applied loads is modified, these being significantly higher (from 100 to 400 kPa), in order to check the deviations in the results of  $k_o$  and  $c_k$  applying the same protocol. Thus, the two successive consolidation tests, steps 8 and 9 (Figure 3), are defined by the following loads:

- First test (step 8): from  $\sigma'_o = 100$  kPa to  $\sigma'_1 = 2\sigma'_o = 200$  kPa.
- Second test (step 9): from  $\sigma'_1 = 200$  kPa to  $\sigma'_2 = 2\sigma'_1 = 400$  kPa.

As in the previous application, we get the characteristic time of each stage ( $\tau_{0,9}$ ) from the consolidation curves (Figures 5 and 6), which are 100 and 85 min for steps 8 and 9, respectively.

In the same way, based on the consolidation curves and from the initial values  $H_o$  and  $e_o$ , we determine the final values of the void ratio ( $e_f$ ) and, by extension, of  $C_c$  for each load step (Table 6).

**Table 6.** Data obtained from compressibility and consolidation curves in clayey soil with muscovite (steps 8 and 9).

Step	$\sigma'_o$ (kPa)	$\sigma'_f$ (kPa)	$S_{100}$ (mm)	$S_i$ (mm)	$S_{prim,cons}$ (mm)	$H_o$ (mm)	$H_f$ (mm)	$e_o$	$e_f$	$C_c$	$\tau_{0,9}$ (s)
8	100	200	-1.225	-0.164	-1.061	7.430	6.899	0.746	0.621	0.414	6000
9	200	400	-1.210	-0.045	-1.165	6.855	6.273	0.611	0.474	0.455	5100

We now repeat the calculation protocol, starting for this second application with an initial value of hydraulic conductivity  $k_{o,I} = 10^{-8}$  m/s. Table 7 shows the intermediate data of the initial

conductivity, permeability index and functional along the 17 iterations necessary for the convergence of the calculation process on this occasion.

**Table 7.** Second application. Partial results of  $k_{o,I}$ ,  $c_{k,I}$  and  $\Theta_I$  throughout the iteration process.

Iteration	$k_{o,I}$ (m/s)	$c_{k,I}$	$\Theta_I$	Iteration	$k_{o,I}$ (m/s)	$c_{k,I}$	$\Theta_I$
01	$1.0000 \times 10^{-8}$	0.0439	828.2885	07	$6.0000 \times 10^{-11}$	0.2683	2.1090
02	$1.0000 \times 10^{-9}$	0.0704	56.3173	08	$5.0000 \times 10^{-11}$	0.3280	1.7047
03	$1.0000 \times 10^{-10}$	0.1776	3.8292	09	$4.0000 \times 10^{-11}$	0.4511	1.3137
04	$9.0000 \times 10^{-11}$	0.1909	3.3859	10	$3.6000 \times 10^{-11}$	0.5482	1.1616
05	$8.0000 \times 10^{-11}$	0.2083	2.9509	11	$3.2000 \times 10^{-11}$	0.7219	1.0124
06	$7.0000 \times 10^{-11}$	0.2324	2.5249	12	$3.1680 \times 10^{-11}$	0.7419	1.0006

Finally, Table 8 summarizes the values obtained for  $c_k$  and the different hydraulic conductivities of the soil ( $k_o$ ,  $k_1$  and  $k_2$ ) in loading stages 8 and 9.

**Table 8.** Second application.  $c_k$  and initial and final hydraulic conductivities for loading steps 8 and 9.

$k_{o,step 8}$ (m/s)	$k_{f,step 8} = k_{o,step 9}$ (m/s)	$k_{f,step 9}$ (m/s)	$c_k$
$3.168 \times 10^{-11}$	$2.152 \times 10^{-11}$	$1.407 \times 10^{-11}$	0.742

#### 4.2. Applications on Kaolinite

For this second soil, two applications of the calculation protocol were carried out. Since the oedometer test consisted of the same 11 loading steps as for the first soil, the intervals chosen for the determination of  $k_o$  and  $c_k$  were the same. This is: between 25 and 100 kPa for low levels of effective stress (third application) and between 100 and 400 kPa for medium-high levels (fourth application).

For the third application, the sample was subjected to the following loads:

- First test (step 2): from  $\sigma'_o = 25$  kPa to  $\sigma'_1 = 2\sigma'_o = 50$  kPa.
- Second test (step 3): from  $\sigma'_1 = 50$  kPa to  $\sigma'_2 = 2\sigma'_1 = 100$  kPa.

While for the fourth application, the load steps were:

- First test (step 8): from  $\sigma'_o = 100$  kPa to  $\sigma'_1 = 2\sigma'_o = 200$  kPa.
- Second test (step 9): from  $\sigma'_1 = 200$  kPa to  $\sigma'_2 = 2\sigma'_1 = 400$  kPa.

As in the previous applications, we got the characteristic time of each stage ( $\tau_{0,9}$ ) from the respective consolidation curves, which were 5.5 and 3.75 min for steps 2 and 3, and 3.2 and 2.7 min for steps 8 and 9. Immediate settlements ( $S_i$ ) and primary consolidation settlements ( $S_{prim,cons}$ ) were also obtained and, from the values of the initial void ratio  $e_{o,r}$  of Table 2 and the oedometric curve of Figure 4, we determined the final values of the void ratios ( $e_o$ ,  $e_f$ ) and, by extension, of  $C_c$  for each loading step (Table 9).

**Table 9.** Data obtained from compressibility and consolidation curves in kaolinite (steps 2–3 and 8–9).

Step	$\sigma'_o$ (kPa)	$\sigma'_f$ (kPa)	$S_{100}$ (mm)	$S_i$ (mm)	$S_{prim,cons}$ (mm)	$H_o$ (mm)	$H_f$ (mm)	$e_o$	$e_f$	$C_c$	$\tau_{0,9}$ (s)
2	25	50	-0.462	-0.053	-0.409	9.085	8.881	1.011	0.966	0.150	330
3	50	100	-0.541	-0.077	-0.464	8.820	8.588	0.952	0.901	0.171	225
8	100	200	-0.501	-0.062	-0.439	8.489	8.269	0.879	0.831	0.161	192
9	200	400	-0.598	-0.051	-0.547	8.205	7.932	0.816	0.756	0.201	162

On this occasion, in the calculation protocol for the third application (steps 2 and 3) we started with an initial value of hydraulic conductivity  $k_{o,I} = 10^{-7}$  m/s, while for the fourth application (steps 8 and 9),  $k_{o,I}$  took the initial value of  $10^{-8}$  m/s. Finally, Tables 10 and 11 summarize the values obtained

for  $c_k$  and the different hydraulic conductivities of the soil ( $k_o$ ,  $k_1$  and  $k_2$ ) in loading stages 2–3 and 8–9, as well as the number of iterations that were necessary in each case.

**Table 10.** Third application.  $c_k$  and initial and final hydraulic conductivities for loading steps 2 and 3.

$k_{o,step\ 2}$ (m/s)	$k_{f,step\ 2} = k_{o,step\ 3}$ (m/s)	$k_{f,step\ 3}$ (m/s)	$c_k$	Iterations
$7.793 \times 10^{-10}$	$6.601 \times 10^{-10}$	$5.468 \times 10^{-10}$	0.628	12

**Table 11.** Fourth application.  $c_k$  and initial and final hydraulic conductivities for loading steps 8 and 9.

$k_{o,step\ 8}$ (m/s)	$k_{f,step\ 8} = k_{o,step\ 9}$ (m/s)	$k_{f,step\ 9}$ (m/s)	$c_k$	Iterations
$3.868 \times 10^{-10}$	$3.024 \times 10^{-10}$	$2.225 \times 10^{-10}$	0.454	14

### 4.3. Comparison, Discussion and Scope of Validity of the Results

A summary of the results obtained for the variables  $k_o$  and  $c_k$  obtained after application of the inverse method proposed in this work is presented in Table 12. The results obtained for tested samples show, without a doubt, the enormous strength and precision of the methodology. On the one hand, both the values of  $k_o$  and  $c_k$ , for each and every one of the load steps analyzed, are within the usual range of these constitutive parameters, referred for this soils by other authors [28–30]. In addition, permeability tests were carried out in a hydraulic cell [27] for these same materials, thus estimating the constitutive permeability parameters  $c_k$  and  $k_o$  (Table 13), which fell close to the orders of magnitude now obtained with our methodology.

**Table 12.** Results of  $c_k$  and  $k_o$  of each application.

Application	Soil	Loading Step	$\sigma'_o - \sigma'_f$ (kPa)	$c_k$	$k_o$ (m/s)	$k_f$ (m/s)
1	Clayey soil with muscovite	2	25–50	0.509	$1.840 \times 10^{-10}$	$9.077 \times 10^{-11}$
		3	50–100		$9.077 \times 10^{-11}$	$4.875 \times 10^{-11}$
2	Clayey soil with muscovite	8	100–200	0.742	$3.168 \times 10^{-11}$	$2.152 \times 10^{-11}$
		9	200–400		$2.152 \times 10^{-11}$	$1.407 \times 10^{-11}$
3	Kaolinite	2	25–50	0.628	$7.793 \times 10^{-10}$	$6.601 \times 10^{-10}$
		3	50–100		$6.601 \times 10^{-10}$	$5.468 \times 10^{-10}$
4	Kaolinite	8	100–200	0.454	$3.868 \times 10^{-10}$	$3.024 \times 10^{-10}$
		9	200–400		$3.024 \times 10^{-10}$	$2.225 \times 10^{-10}$

**Table 13.** Constitutive permeability parameters  $c_k$  and  $k_o$  for the two soils. Data obtained from tests with hydraulic cells.

$\sigma'$ (kPa).	Clayey Soil with Muscovite			Kaolinite		
	e	k (m/s)	Averaged $c_k$	e	k (m/s)	Averaged $c_k$
25	1.121	$3.122 \times 10^{-10}$	0.568	1.04	$1.134 \times 10^{-9}$	0.528
50	0.943	$1.167 \times 10^{-10}$		0.973	$8.678 \times 10^{-10}$	
100	0.758	$6.432 \times 10^{-11}$		0.874	$5.988 \times 10^{-10}$	
200	0.602	$3.743 \times 10^{-11}$		0.797	$4.233 \times 10^{-10}$	
400	0.456	$1.855 \times 10^{-11}$		0.728	$2.876 \times 10^{-10}$	

On the other hand, the comparison between the results obtained in the first two applications (made for the same soil, that with a high content of muscovite) cannot be more conclusive, namely: the value of  $k$  for an effective stress of 100 kPa, both in the final stretch of step 3 (50–100 kPa) and in the initial stretch of step 8 (100–200 kPa), is practically the same and the difference found can be attributed to the effects of creep. Regarding the value of  $c_k$ , it is true that slight differences were found for the value of this parameter in each of the stress ranges tested (0.509 for low levels of effective stress, 0.742 for medium-high levels). However, it is important to keep in mind that the results obtained come directly from real laboratory data, with the addition of being different loading levels, so that,

in reality, we can consider that the determinations are correct. In practice, the engineer who uses this methodology could choose between taking the permeability index corresponding to the stress level closest to his real case study or taking the average value ( $c_k = 0.626$ ).

The same conclusions can be drawn from the results obtained in the second two applications, carried out on kaolinite. In this sense, it should be noted, mainly, that it is a soil that has given much shorter consolidation times in the oedometer (in the order of 10 to 20 times lower) than the first sample. Therefore, we can affirm that the calculation protocol presented here (and which is based, in turn, on a general non-linear consolidation model [15]) can be successfully applied to a large group of fine-grained soils (percentage of fines above 35%), such as clays, silts and mixtures of fine sands, silts and clays (here we can include both soils with medium-low plasticity ( $20 < LL < 50$ ) and soils with high plasticity, provided that LL values above 100 are not exceeded). Perhaps, the only limitation that the methodology presented here may have is found neither in the non-linear consolidation model nor in the calculation protocol, but in the oedometer test itself, since in this, due to the use confining rings of small thickness (20 mm in the case presented here), soils with hydraulic conductivity values above  $10^{-8}$  m/s could present very fast consolidation processes, which would greatly hinder the correct obtaining of the consolidation time  $\tau_{0.9}$ . In any case, the compressibility of the material is also an important factor that affects the greater or lesser speed of consolidation of these soils.

#### 4.4. Influence of Measurement Errors

In order to study the influence of errors, coming from the measurement of the characteristic consolidation times ( $\tau_{0.9,1}$  and  $\tau_{0.9,2}$ ) and compression indexes ( $C_{c,1}$  and  $C_{c,2}$ ) of the oedometer test, in the solution of the final magnitudes  $k_o$  and  $c_k$ , we will proceed as follows. Taking both soils used in the applications of the previous section, we introduce an error  $\xi$  ( $\pm 0.5, 1$  and  $2\%$ ) in the magnitudes ( $\tau_{0.9,1}$ ,  $\tau_{0.9,2}$ ,  $C_{c,1}$  and  $C_{c,2}$ ) which will lead to a set of experimental value groups  $\tau_{0.9,1,\xi}$ ,  $\tau_{0.9,2,\xi}$ ,  $C_{c,1,\xi}$  and  $C_{c,2,\xi}$ . From these measurements, the deviations of  $k_o$  and  $c_k$  associated with each value of  $\xi$  are determined. The results are shown in Tables 14 and 15 and in Figure 9 (with a fitting curve). It can be seen how, for errors in experimental measurements of even  $2\%$ , the deviations in the estimates of  $k_o$  and  $c_k$  are below  $20\%$ . It is, therefore, a very reliable determination, especially if we take into account that in the field of geotechnical engineering the usual errors in  $k_o$  come to establish ranges of acceptable values confined between one or even two orders of magnitude.

**Table 14.** Maximum errors of  $k_o$  and  $c_k$  as a function of  $\xi$  (high muscovite content soil).

Steps	$C_c$ and $\tau_{0.9}$	Rel. Error $\xi$ (%)	$k_o$ Max. Rel. Error (%)	$c_k$ Max. Rel. Error (%)
2–3		0.5	3.63	4.07
		1.0	7.47	8.56
		2.0	15.37	18.33
8–9		0.5	3.48	3.99
		1.0	7.36	8.14
		2.0	15.11	17.35

**Table 15.** Maximum errors of  $k_o$  and  $c_k$  as a function of  $\xi$  (kaolinite).

Steps	$C_c$ and $\tau_{0.9}$	Rel. Error $\xi$ (%)	$k_o$ Max. Rel. Error (%)	$c_k$ Max. Rel. Error (%)
2–3		0.5	3.86	4.01
		1.0	7.71	8.31
		2.0	15.88	17.91
8–9		0.5	3.62	3.84
		1.0	7.61	7.97
		2.0	15.34	17.14

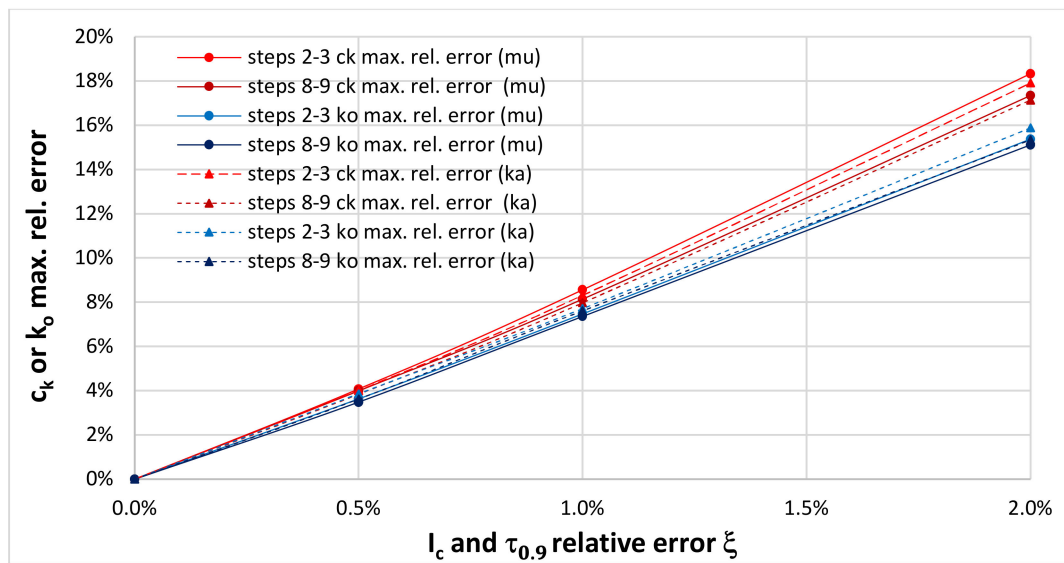


Figure 9. Maximum deviations of  $k_0$  and  $c_k$  as a function of  $\xi$ .

In general, the errors that determine the values of the affected experimental data  $\tau_{0.9,1,\xi}$ ,  $\tau_{0.9,2,\xi}$ ,  $C_{c,1,\xi}$  and  $C_{c,2,\xi}$  are random and alter the exact values above or below. This, together with the application of two successive processes of calculation or resolution of Equations (12) and (3), one for each stage of consolidation, almost assures an accentuated partial compensation between errors. In fact, making a total of 1000 simulations with a random error of 2%, the previous maximum error of 18.91% (Tables 14 and 15) has been reduced to 3.36%, a more than acceptable result in this engineering problem.

#### 4.5. Final Comments on the Protocol

In the presented methodology there can be other possibilities or criteria when taking the soil parameters necessary for the application of the inverse problem through the universal curve  $\pi_I = \Psi(\pi_{II})$ . Thus, as we have commented in the applications section, it is necessary to adopt a criterion to determine the value of the final void ratio in the consolidation curve, a data from which we obtain the characteristic consolidation time, in which 90% of the final settlement is reached. Although the value of the final void ratio will not vary greatly, since creep deformation in the oedometer test is not significant, this can happen with the characteristic consolidation time  $\tau_{0.9}$ , so the determination of this last parameter is essential to make a good estimate of the constitutive permeability parameters sought.

Also, in the choice of the value of  $C_c$  different criteria can be taken from the one adopted here. For each of the two applications shown we have taken the value of  $C_c$  derived from each loading stage, although an average of these could also have been chosen (for steps 2 and 3, on the one hand, and for steps 8 and 9, on the other) or even a general averaged value. In any case, these values are all very close and the differences found would not be large, as we have seen in the section dedicated to error evaluation.

The adjustment of the relation  $\pi_I = \Psi(\pi_{II})$  proposed by Equation (12) is good enough ( $R^2 = 0.998$ ) to justify the use of this equation in the whole range of values of  $\pi_{II}$ . It is true that this expression could be used to make a first estimation of  $c_k$  and, from the value of this parameter, choose one of the Equations (13)–(15) to repeat the process and obtain a definitive result. In any case, the differences found would not be significant and the use of Equation (12) is presented as a sufficiently precise option.

The methodology presented here also does not require a loading ratio of 2 between successive steps, but here it has been taken with the intention of illustrating that an oedometer test according to the standards [26,31] can be used, without the need to make variations or modifications on it. The results obtained with other loading ratios would lead to equally accurate results, only depending on the aforementioned measurement errors of the experimental data.

In view of the consolidation Equation (8), which governs the non-linear model of Alhama et al. [15], and the dimensionless groups (10) with which the universal solutions for the characteristic time are constructed, the present methodology could be applied for unloading phases or even for overconsolidated soils (as long as the preconsolidation pressure is not exceeded). In this sense, the compression index to be obtained and entered in the calculation protocol would be that corresponding to the unload-reload branch of the oedometric curve, while the permeability index obtained would obviously be that corresponding to an overconsolidated soil. In any case, for this, it would be necessary to obtain previously the unknown function  $\Psi$  that would relate the monomials  $\pi_I$  and  $\pi_{II}$  under conditions of overconsolidated soil, based on numerical simulations similar to those of the work of Alhama et al. [15].

## 5. Conclusions

The procedure proposed in this work allows to obtain in a simple and precise way the non-linear constitutive parameters of consolidation  $k_o$  and  $c_k$  by means of a simple oedometer test and the use of the universal curves of characteristic time of consolidation obtained by the authors in a recent work.

The computation times, usually high in this type of inverse problems, are reduced to a negligible value thanks to the use of these curves by means of a calculation routine of easy programming.

The applications carried out from real oedometer tests on two fine-grained soils with different properties show the accuracy of the methodology. On the one hand, the results obtained for  $k_o$  and  $c_k$  are consistent with the values referred by other authors for samples of similar characteristics and for any range of stress considered. On the other hand, both the  $c_k$  and  $C_c$  values for the two applications carried out on each sample (one for low stress levels and one for medium-high levels) are very close, which shows the robustness of the procedure, in which real laboratory data have been strictly used, without any mathematical manipulation. In addition, in each pair of applications the samples were subjected to a vertical stress of 100 kPa (end of the 25–50–100 kPa loading stretches and beginning, after two unloading-reloading phases, of the 100–200–400 kPa loading stretches) and, in both cases, with completely independent oedometer test data, the hydraulic conductivity values determined by the inverse calculation protocol were practically the same.

The calculation protocol presented here can be successfully applied to a large group of fine-grained soils, such as clays, silts and mixtures of these with fine sands, with the only limitation found in the oedometer test itself, where the small thickness of the confining ring can lead to very fast consolidation processes in soils with high hydraulic conductivity (above  $10^{-8}$  m/s), making it difficult to get the correct consolidation time  $\tau_{0.9}$ .

Finally, it has been found that, for the typical errors in the experimental measurements of the oedometer test (up to 2%), the deviations in the parameters  $c_k$  and  $k_o$  can be considered small and very acceptable in this field of engineering.

**Author Contributions:** Conceptualization, G.G.-R. and I.A.; methodology, G.G.-R. and I.A.; software, G.G.-R.; validation, G.G.-R. and I.A.; formal analysis, G.G.-R. and I.A.; investigation, G.G.-R. and I.A.; writing—original draft preparation, G.G.-R.; writing—review and editing, G.G.-R.; visualization, G.G.-R.; supervision, G.G.-R. and I.A. All authors have read and agreed to the published version of the manuscript.

**Funding:** This research received no external funding.

**Conflicts of Interest:** The authors declare no conflict of interest

## Nomenclature

$C_c$	compression index
$C_{c,1}, C_{c,2}$	compression index of successive consolidation steps
$c_k$	permeability index
$dz$	differential element length (m)
$dz_0$	initial differential element length (m)
$e$	void ratio
$e_1, e_2$	final void ratios of the two successive consolidation steps
$e_f$	final void ratio
$e_0$	initial void ratio
$e_{0,oed}$	void ratio for effective reconsolidation stress of a remoulded sample
$e_{0,r}$	void ratio of the sample when it is introduced into the confining ring
$G_s$	specific gravity of solids
$H$	draining length of the soil (m)
$H_1, H_2$	final draining lengths of the two successive consolidation steps (m)
$H_f$	final draining length (m)
$H_0$	initial draining length (m)
$k$	hydraulic conductivity (or permeability) (m/s)
$k_1, k_2$	final hydraulic conductivities of the two successive consolidation steps (m/s)
$k_0$	initial hydraulic conductivity (m/s)
$L(10)$	natural logarithm of 10
LL	liquid limit
PI	plasticity index
$S_{100}$	settlement that includes immediate and primary consolidation settlements (m)
$S_i$	immediate settlement (m)
$S_{prim,cons}$	primary consolidation settlement (m)
$t$	time (s)
$u$	excess pore pressure (Pa)
$\gamma_w$	water specific weight (N/m <sup>3</sup> )
$\lambda$	parameter of Cornetti and Battaglio model. $\lambda = 1 - C_c/c_k$
$\pi_I$	dimensionless group that involves, among others, the characteristic settlement time
$\pi_{II}$	dimensionless group that involves, among others, the loading factor
$\sigma_c$	load applied to the soil surface (Pa)
$\sigma'$	effective soil stress (Pa)
$\sigma'_1$	final effective stress of the first consolidation step (Pa)
$\sigma'_2$	final effective stress of the second consolidation step (Pa)
$\sigma'_f$	final effective stress (Pa)
$\sigma'_0$	initial effective stress (Pa)
$\sigma'_{0,oed}$	effective reconsolidation stress for the oedometer test of a remolded soil (Pa)
$\tau_{0,9}$	characteristic time to reach 90% of the final settlement (s)
$\tau_{0,9,1}$	characteristic settlement time of the first loading step (s)
$\tau_{0,9,2}$	characteristic settlement time of the second loading step (s)
$\omega$	differential void ratio
$\Psi$	arbitrary mathematical function
$\Theta$	functional defined by Equation (13)
$\Theta_{ref}$	reference value for the functional $\Theta$

## Subscripts

1,2	denote successive values of the two steps of the test
F	final value of the iterated parameter
$\xi$	denotes the error of an experimental quantity

## References

1. Taylor, D.W. *Fundamentals of Soil Mechanics*. *Soil Sci.* **1948**, *66*, 161. [[CrossRef](#)]
2. Scott, R.F. *Principles of Soils Mechanics*; Addison-Wesley Publishing Company: Reading, MA, USA, 1963.
3. Berry, P.L.; Reid, D. *An Introduction to Soil Mechanics*; McGraw-Hill: London, UK, 1987.
4. García-Ros, G. Caracterización Adimensional y Simulación Numérica de Procesos Lineales y No Lineales de Consolidación de Suelos. Ph.D. Thesis, Universidad Politécnica de Cartagena, Cartagena, Spain, 2016.
5. Davis, E.H.; Raymond, G.P. A non-linear theory of consolidation. *Geotechnique* **1965**, *15*, 161–173. [[CrossRef](#)]
6. Juárez-Badillo, E. General Theory of Consolidation for Clays. *Consol. Soils: Test. Eval.* **1986**, 137–153. [[CrossRef](#)]
7. Cornetti, P.; Battaglio, M. Nonlinear consolidation of soil modeling and solution techniques. *Math. Comput. Model.* **1994**, *20*, 1–12. [[CrossRef](#)]
8. Arnod, S.; Battaglio, M.; Bellomo, N. Nonlinear models in soils consolidation theory parameter sensitivity analysis. *Math. Comput. Model.* **1996**, *24*, 11–20. [[CrossRef](#)]
9. Baral, P.; Rujikiatkamjorn, C.; Indraratna, B.; Leroueil, S.; Yin, J.-H. Radial Consolidation Analysis Using Delayed Consolidation Approach. *J. Geotech. Geoenviron. Eng.* **2019**, *145*, 04019063. [[CrossRef](#)]
10. Bi, G.; Ni, S.; Wang, D.; Chen, Y.; Wei, J.; Gong, W. Creep in Primary Consolidation with Rate of Loading Approach. *Sci. Rep.* **2019**, *9*, 1–9. [[CrossRef](#)]
11. García-Ros, G.; Alhama, I.; Morales, J.L. Numerical simulation of nonlinear consolidation problems by models based on the network method. *Appl. Math. Model.* **2019**, *69*, 604–620. [[CrossRef](#)]
12. Buckingham, E. On physically similar systems; Illustrations of the use of dimensional equations. *Phys. Rev.* **1914**, *4*, 345. [[CrossRef](#)]
13. García-Ros, G.; Alhama, I.; Alhama, F. Dimensionless characterization of the non-linear soil consolidation problem of Davis and Raymond. Extended models and universal curves. *Appl. Math. Nonlinear Sci.* **2019**, *4*, 61–78. [[CrossRef](#)]
14. García-Ros, G.; Alhama, I.; Cánovas, M.; Alhama, F. Derivation of universal curves for nonlinear soil consolidation with potential constitutive dependences. *Math. Probl. Eng.* **2018**, *2018*, 15. [[CrossRef](#)]
15. Alhama Manteca, I.; García-Ros, G.; Alhama López, F. Universal solution for the characteristic time and the degree of settlement in nonlinear soil consolidation scenarios. A deduction based on nondimensionalization. *Commun. Nonlinear Sci. Numer. Simul.* **2018**, *57*, 186–201. [[CrossRef](#)]
16. García-Ros, G.; Alhama, I.; Cánovas, M. Powerful software to Simulate soil Consolidation problems with prefabricated Vertical Drains. *Water* **2018**, *10*, 242. [[CrossRef](#)]
17. García-Ros, G.; Alhama, I.; Cánovas, M. Use of discriminated nondimensionalization in the search of universal solutions for 2-D rectangular and cylindrical consolidation problems. *Open Geosci.* **2018**, *10*, 209–221. [[CrossRef](#)]
18. Sánchez-Pérez, J.F.; Alhama, I. Simultaneous determination of initial porosity and diffusivity of water-saturated reinforced concrete subject to chloride penetration by inverse problem. *Constr. Build. Mater.* **2020**, *259*, 120–412. [[CrossRef](#)]
19. Zueco, J.; Alhama, F. Simultaneous inverse determination of temperature-dependent thermophysical properties in fluids using the network simulation method. *Int. J. Heat Mass Transf.* **2007**, *50*, 3234–3243. [[CrossRef](#)]
20. Beck, J.V.; Blackwell, B.; St Clair, C.R. *Inverse Heat Conduction: Ill.-Posed Problems*; John Wiley and Sons: Hoboken, NJ, USA, 1985.
21. Feizmohammadi, A.; Oksanen, L. An inverse problem for a semi-linear elliptic equation in Riemannian geometries. *J. Differ. Equ.* **2020**, *269*, 4683–4719. [[CrossRef](#)]
22. Burger, M.; Elvetun, O.L.; Schlottbom, M. Diffuse interface methods for inverse problems: Case study for an elliptic Cauchy problem. *Inverse Probl.* **2015**, *31*, 125002. [[CrossRef](#)]
23. Taylor, D.W. *Research on Consolidation of Clays*; Massachusetts Institute of Technology: Cambridge, MA, USA, 1942.
24. Chu, J.; Bo, M.W.; Chang, M.F.; Choa, V. Consolidation and permeability properties of Singapore marine clay. *J. Geotech. Geoenviron. Eng.* **2002**, *128*, 724–732. [[CrossRef](#)]
25. Casagrande, A.; Fadum, R.E. Notes on soil testing for engineering purposes. *Harv. Soil Mech. Ser.* **1940**, *8*, 74.
26. Normalización Española. Parte 5: Ensayo edométrico de carga incremental. In *UNE-EN ISO 17892-5. Investigación y Ensayos Geotécnicos*; Ensayos de Laboratorio de Suelos: Madrid, Spain, 2017; pp. 1–38.

27. British Standards Institution. *BS 1377-6: 1990. Methods of Test for Soils for Civil Engineering Purposes. Consolidation and Permeability Tests in Hydraulic Cells and with Pore Pressure Measurement*; British Standards Institution: London, UK, 1990.
28. Horpibulsuk, S.; Yangsukkaseam, N.; Chinkulkijniwat, A.; Du, Y.J. Compressibility and permeability of Bangkok clay compared with kaolinite and bentonite. *Appl. Clay Sci.* **2011**, *52*, 150–159. [[CrossRef](#)]
29. Veess, E.; Winterkorn, H.F. Engineering properties of several pure clays as functions of mineral type, exchange ions and phase composition. *Highw. Res. Rec.* **1967**, *209*, 55–65.
30. Abbasi, N.; Rahimi, H.; Javadi, A.A.; Fakher, A. Finite difference approach for consolidation with variable compressibility and permeability. *Comput. Geotech.* **2007**, *34*, 41–52. [[CrossRef](#)]
31. British Standards Institution. *BS 1377-5: 1990. Methods of Test for Soils for Civil Engineering Purposes—Part 5: Compressibility, Permeability and Durability Tests*; British Standards Institution: London, UK, 1990; 36p.

**Publisher's Note:** MDPI stays neutral with regard to jurisdictional claims in published maps and institutional affiliations.



© 2020 by the authors. Licensee MDPI, Basel, Switzerland. This article is an open access article distributed under the terms and conditions of the Creative Commons Attribution (CC BY) license (<http://creativecommons.org/licenses/by/4.0/>).